https://doi.org/10.5194/egusphere-2025-710
Preprint. Discussion started: 15 April 2025


# Linear Meta-Model optimization for regional climate models (LiMMo version 1.0)

Sergei Petrov[1], Andreas Will[2], and Beate Geyer[1]

[1]Institute of Coastal Systems, Helmholtz-Zentrum Hereon, Germany
[2]Atmospheric Processes, BTU Cottbus-Senftenberg, Germany

**Correspondence:** Sergei Petrov (sergei.petrov@hereon.de)

**Abstract.** A new tool for objective parameter tuning of regional climate models is presented. The climate model output was emulated using a linear regression approach for each grid point on a monthly mean basis (Linear Meta-Model – LiMMo). This linear approximation showed high accuracy over a 6-year period. The error norm between the Meta-Model and the observational data sets was minimized using the gradient-based, limited-memory Broyden-Fletcher-Goldfarb-Shanno method with box constraints. The LiMMo framework was applied to the state-of-the-art regional climate model ICON-CLM, tuned to the E-OBS and HOAPS observational data sets. Different optimization objectives were explored by assigning varying weights to model variables in the error norm definition. The combination of a linear emulator with fast gradient-based optimization allows the proposed method to scale linearly with the number of model variables and parameters, facilitating the tuning of dozens of parameters simultaneously.

## 1 Introduction

In environmental modeling, the tuning process aims to identify the set of model parameters that minimize the discrepancy between model outputs and observational data. This process is crucial across various fields of numerical weather and climate modeling, from short-range numerical weather prediction to global and regional climate simulations. Examples of such tuning efforts are the optimization of the Max Planck Institute Earth System Model (Mauritsen and Roeckner, 2020) and the adaptive adjustment of uncertain parameters in ICON, the operational forecast system of the German Weather Service (Zängl, 2023). When new parameterizations are introduced, re-tuning is often required to find the optimal combination of old and new parameters for the updated configuration. As more accurate observational data sets become available, they must also be incorporated into the tuning framework. This emphasizes the need for robust and computationally efficient tuning tools to ensure that evolving environmental models remain consistent with improving observational data sets.

The tuning of regional climate models is a computationally intensive and time-consuming process. Conducting a single decadal simulation of a high-resolution regional climate model (spatial resolution of approximately 10–20 km) for the Europe domain typically requires several days on high-performance computing systems. A viable approach to mitigating this challenge is the development of approximations to dynamical simulations, often referred to as "emulators" or "Meta-Models". These Meta-Models are computationally much cheaper than the dynamic simulations. Once a Meta-Model is established, an

https://doi.org/10.5194/egusphere-2025-710
Preprint. Discussion started: 15 April 2025


optimization process can be employed to identify parameter sets that minimize the spatially and temporally aggregated bias of the Meta-Model relative to observational data. This approach is referred as objective tuning, or objective calibration. Consistent with prior studies (Gregoire et al., 2011; Bellprat et al., 2015; Avgoustoglou et al., 2022), we adopt a regression-based Meta-Model for each grid point and time step, providing a straightforward yet effective solution.

An important limitation is usually the size of the training data set required to create the statistical model. The Meta-Model is trained on climate model outputs. For quadratic regression (proposed in (Neelin et al., 2010) and utilized in (Bellprat et al., 2015; Avgoustoglou et al., 2022)), the minimum number of required dynamic simulations is given by $(2N+1)+\frac{N\cdot(N-1)}{2}$, where $N$ is the number of parameters considered - 3 simulations along each parameter axis and one simulation for each parameter pair. The number of simulations required grows as $N^2$, which makes the training of quadratic regression impractically time-consuming as one has to conduct the dynamical simulation for each pair of parameters. Therefore, we propose the linear regression approach, which requires only $N+1$ dynamic simulations - only 2 for each parameter perturbation (if the reference simulation is fixed - only 1). As will be shown later, the linear approach achieves good accuracy for most variables and could be used as a simple and fast emulator.

Another critical aspect of objective tuning is the choice of optimization technique. So far, Monte Carlo-based optimization has been the primary method proposed. While this approach is effective in certain contexts, it suffers from significant accuracy and scalability limitations as it requires an exponentially increasing number of samples with the dimensionality of the parameter space. It is well established that the minimum number of Latin Hypercube samples required to outperform random sampling is $6^d$ (Morokoff and Caflisch, 1995), where $d$ denotes the dimensionality of the parameter space. For instance, in a parameter space with 12 dimensions, Monte Carlo optimization would require at least $6^{12} \approx 2 \cdot 10^9$ evaluations of the error norm. Assuming that each evaluation takes approximately 1 second (which was the case for our code), the total computation time on 1000 CPU cores would amount to about one month, assuming perfect parallel scaling. This computational cost is impractically high and highlights the need for more efficient optimization strategies.

In contrast, the current study introduces a gradient-based optimization method for objective tuning for the first time. By maintaining a relatively simple objective function (Root Mean Square Error), it becomes possible to derive an analytical expression for the gradient and implement a fast evaluation procedure. Consequently, the overall execution time for gradient-based optimization is significantly reduced compared to the Monte Carlo approach. Gradient-based optimization scales linearly with the number of parameters and variables considered and achieves the perfect accuracy with very limited number of iterations. This efficiency gain enables the consideration of dozens of parameters.

The combination of a simplified statistical emulator, where linear regression requires only a single parameter disturbance simulations, with a fast gradient-based optimization method enables the calibration of regional climate models in less than one hour without the need for parallelization for dozens of parameters. In addition, this study also introduces the concept of optimizing constant shifts related to discrete logical conditions (e.g., the choice of external data sets of orography and aerosol), assuming that their impact on continuous parameters is minimal. By applying linear regression with constant shifts, the influence of interaction terms between the parameters is excluded.

https://doi.org/10.5194/egusphere-2025-710
Preprint. Discussion started: 15 April 2025


Due to the high computational costs involved in obtaining the optimization results, previous studies (Neelin et al., 2010; Bellprat et al., 2015; Avgoustoglou et al., 2022) lacked an investigation into the influence of the optimization results on the definition of the tuning score. The LiMMo framework, however, provides significant flexibility that allows users to customize the tuning process according to their specific goals. Users can select different model variables, continuous and logical parameters, and gridded observation data sets. Ultimately, the scalar error norm function is minimized, requiring the user to define the optimization objective by assigning appropriate weights to the model variables. The selection of weights can lead to different optimal configurations tailored to specific applications.

For instance, predicting extreme flood events would require assigning the highest weight to precipitation. For reliable climate predictions in the assessment of renewable energy, greater weights should be given to short-wave radiation (relevant for the performance of solar panels) and wind speed (crucial for the operation of wind farms). Similarly, if the focus is on the accurate prediction of heat waves, the weighting of temperature variables should be increased. This flexibility allows the framework to effectively cover a wide range of applications and user-specific objectives.

The following text is divided into four sections. The **methodology** (section 2) outlines the most important aspects of the proposed framework. The **results** of the optimization are presented in section 3. **Discussion** in section 4 covers aspects of tuning that fall outside the scope of the current study. Finally, the most important results are highlighted in **conclusions** (section 5).

## 2 Methodology

In this section, we provide a detailed description of the LiMMo framework, which was developed during the tuning process of the ICON-CLM regional climate model (Pham et al., 2021). The model was configured at a 12-km spatial resolution over the EURO-CORDEX domain (Jacob et al., 2014) and optimized against observational data.

The list of considered model quantities is presented in section 2.1. Details of the observational data sets are provided in section 2.2. The setup of the regional climate model ICON-CLM is described in section 2.3, while the list of ICON-CLM tuning parameters is outlined in section 2.4. The definition of the error norm relative to observations, which serves as the optimization objective, is discussed in section 2.5. The Meta-Model approximation methodology is explained in section 2.6. Finally, the proposed gradient-based optimization method is described in section 2.7.

### 2.1 Model quantities

The following seven surface prognosic variables are considered in this study:

- **tas**, hourly mean 2-meter temperature (deg $K$);
- **rsds**, hourly mean downward net shortwave radiation flux, ($W \cdot m^{-2}$);
- **tasmin**, daily minimum 2-meter temperature (deg $K$);
- **tasmax**, daily maximum 2-meter temperature (deg $K$);

https://doi.org/10.5194/egusphere-2025-710
Preprint. Discussion started: 15 April 2025


- **psl**, hourly mean atmospheric pressure at the surface ($Pa$);
- **pr_amount**, hourly total amount of precipitations ($mm$ per $h$);
- **hfls**, hourly mean surface downward latent heat flux ($W \cdot m^{-2}$).

The selection of variables can be adjusted according to the user's interests. In addition to the commonly analyzed variables (**tas**, **tasmin**, **tasmax**, **pr_amount**, **psl**), we include the latent heat flux (**hfls**) due to its significant influence on long-term precipitation formation via evaporation over the sea. The 2D quantities from the list were extracted from both climate model output and observational data sets for the tuning period from January 1, 2003 to December 31, 2008.

### 2.2 Observational data sets

As a reference for **tas**, **rsds**, **tasmin**, **tasmax**, **psl**, and **pr_amount**, the E-OBS version 29.0 data set (Cornes et al., 2018) was selected. It provides high quality daily data over Europe with a spatial resolution of about 25 km and a temporal coverage since 1950. With its fine spatial detail, daily temporal resolution, and ensemble-based uncertainty estimates, E-OBS is a robust resource for analyzing regional climate variability, long-term trends, and making reliable climate assessments.

We aim to tune the **hfls** to align with the HOAPS version 4.0 data set (Andersson et al., 2010). HOAPS provides a satellite-based climatology of latent heat flux over the global ice-free oceans, derived from recalibrated SSM/I and SSMIS sensor measurements. It covers the period from 1987 to 2014 with a spatial resolution of about 55 km and provides 6-hourly averages. Using the COARE bulk flux algorithm, HOAPS provides accurate estimates, making it a key reference for ocean-atmosphere interaction studies and energy exchange assessments.

Temporally averaged surface fields of **tasmin**, **tasmax**, **rsds**, **pr_amount**, **psl**, and **hfls** interpolated to the climate model output grid are shown in Fig.1 for the tuning period 2003-2008.

### 2.3 Regional climate model ICON-CLM

ICON is a state-of-the-art model for global circulation modeling, Regional Climate Modeling (RCM), operational Numerical Weather Prediction (NWP), Large Eddy Simulations (LES), and environmental prediction (Zängl et al., 2015; Klocke et al., 2017; Stevens et al., 2017). The model is available since 2024. It uses an unstructured triangular grid, allowing nearly uniform resolution across the globe at any grid scale. The model is capable of simulations down to sub-kilometer scales, with common dynamics and numerics across all application modes. The model physics, however, differs between applications, with specific versions for Earth system modeling, NWP/RCM, and LES.

ICON-CLM (ICON in Climate Limited-area Mode) is the configuration used for RCM applications. It utilizes NWP physics with climate-specific extensions for long-term simulations. The first version of ICON-CLM is based on ICON release 2.6.1 (Pham et al., 2021). Typically, it operates in a one-way nesting mode, with coarse grid lateral boundary conditions and bottom boundary conditions over oceans. In the current study, Rayleigh damping is applied at the upper boundary to handle gravity waves.

https://doi.org/10.5194/egusphere-2025-710
Preprint. Discussion started: 15 April 2025


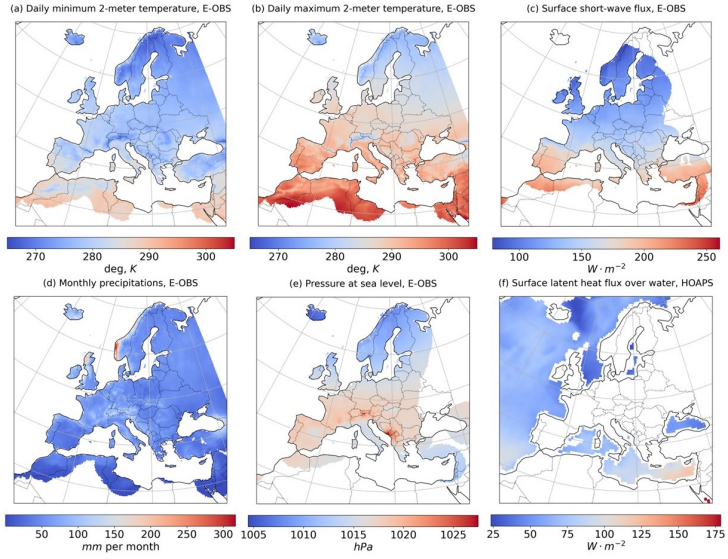


**Figure 1.** 2003-2008 mean observations: (a) daily minimum 2-meter temperature, E-OBS; (b) daily maximum 2-meter temperature, E-OBS; (c) daily mean short-wave radiation flux, E-OBS; (d) total monthly precipitations, E-OBS; (e) daily mean atmostperic pressure at sea level, E-OBS; (f) daily mean latent heat flux over water, HOAPS.

The ICON release model version from 2024.07 (ICON partnership (DWD, MPI-M, DKRZ, KIT, C2SM), 2024) is used with the ERA5 reanalysis (Hersbach et al., 2020) boundary conditions for the period 2003-2008. The simulation grid R13B5 (ICON terminology) corresponds to a mesh size of about 12.14 km. As a post-processing step, the model fields were interpolated onto a rotated 412 × 424 rectangular grid of the EURO-CORDEX model domain (Fig. 2) with a spatial resolution of 12 km, ensuring convenient data storage and accessibility for analysis.

### 2.4 Tuning parameters of ICON-CLM

In this study, 15 parameters are selected for optimization, which is twice the number of parameters used in applications of the weakly non-linear Meta-Model approach (Bellprat et al., 2015; Avgoustoglou et al., 2022). The following subsections discuss the physical meaning and relevance of these parameters. All model parameters are grouped into four categories. A brief description of the **Surface Transfer Scheme** (section 2.4.1) and **Mixing in the Planetary Boundary Layer** (section 2.4.2) parameters is given in Tab. A1 in the Appendix. Descriptions of the **Cloud Cover** (section 2.4.3) and **External Data sets** (section 2.4.4) parameters can be found in Tab. A2. For more details, please refer to the ICON namelist parameter overview (https://gitlab.dkrz.de/icon/icon-model/-/blob/release-2024.07-public/doc/Namelist_overview.pdf).

The ICON namelist parameter names are designed to be self-explanatory, but this often results in them being quite long. To address this, the tables in the appendix (Tab. A1 and Tab. A2) provide a mapping between the full ICON parameter names and the shorter versions used in the current study. In the text, ICON parameter names are highlighted with `mono-space`

https://doi.org/10.5194/egusphere-2025-710
Preprint. Discussion started: 15 April 2025


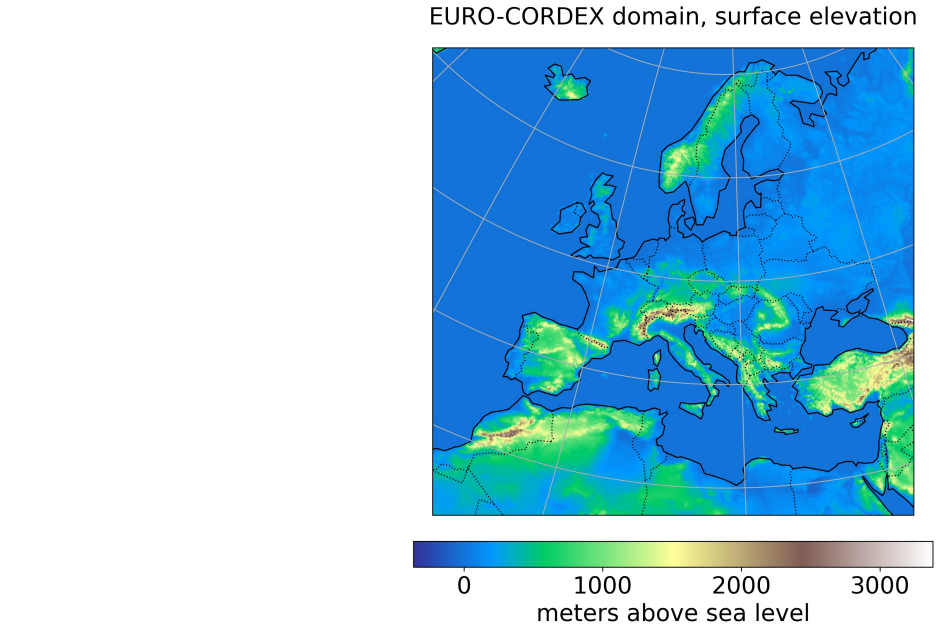


**Figure 2.** EURO-CORDEX domain, height of the Earths surface above sea level.

font, while the corresponding short acronyms are highlighted with **bold** font. For example, the ICON parameter for the relative humidity range is `tune_box_liq`, which corresponds to the acronym **tbl**.

### 2.4.1 Surface Transfer Scheme

The surface transfer scheme contains several tuning parameters, some of which are known to significantly impact near-surface climate conditions. These parameters, along with several related and newly introduced ones, are used for optimization. Specifically, the parameters `rlam_heat`, `rat_sea`, `cr_bsmin`, and `rsmin_fac` have been identified as particularly sensitive in climate modeling. Even small changes within their uncertainty ranges can lead to substantial changes in the simulated climate, particularly in the near-surface air temperature (**tas**). These parameters have been optimized in previous studies (Bellprat et al., 2015; Avgoustoglou et al., 2022).

The parameters `rlam_heat` and `rat_sea`, along with the newly introduced parameter `rat_lam`, serve to scale the resistance to latent and sensible heat flux over both land and sea surfaces, as described in the Tab. 1.

| | **Land** | **Sea** |
|---|---|---|
| **Latent Heat Flux** | `rlam_heat` · `rat_lam` | `rlam_heat` · `rat_sea` |
| **Sensible Heat Flux** | `rlam_heat` | `rlam_heat` · `rat_sea` |

**Table 1.** Influence of the parameters `rlam_heat`, `rat_sea`, and `rat_lam` on the latent and sensible heat fluxes.

https://doi.org/10.5194/egusphere-2025-710
Preprint. Discussion started: 15 April 2025


These parameters provide the flexibility to tune the heat fluxes over land and sea surfaces independently, and allow the adjustment of the Bowen ratio over land surfaces.

The parameters `cr_bsmin` and `rsmin_fac` represent the minimum resistance to evaporation from bare soil, relevant for wet soil conditions, and the scaling factor for the minimum resistance of plant transpiration, respectively. These minimum resistances limit evapotranspiration and are known to have a significant impact on soil moisture. Consequently, they influence the annual cycle climatologies, especially with respect to soil moisture dynamics.

Recently, the parameter pair `tune_albedo_wso` = (**taw1**, **taw2**) was introduced to correct the reference albedo for dry (**taw1**) and wet (**taw2**) soil conditions. This parameterization was initially motivated by the model's warm **tas** bias in the Mediterranean and cold bias in central and northern Europe. Additionally, it accounts for the fact that observed albedo tends to be reduced for wet soils and increased for very dry soils.

### 2.4.2 Mixing in the Planetary Boundary Layer

The parameters `tkhmin` and `tkmmin` represent the minimum diffusion coefficients for vertical mixing of heat and momentum, respectively. They maintain mixing under opaque cloud cover and help dissolve the clouds, compensating for the excessive effective viscosity caused by numerical diffusion, which dampens instabilities. However, this minimum diffusion can keep mixing too high in stable, low-turbulence conditions, especially in winter, leading to excessively warm near-surface temperatures. These parameters should be as low as possible, but high enough to be effective, and have previously been optimized by expert judgment or objective calibration (Avgoustoglou et al., 2022). In this study, `tkhmin` and `tkmmin` are tuned simultaneously with the same factor (later the same acronym **tkhmin** is used for `tkhmin` = `tkmmin`).

### 2.4.3 Cloud Cover

The cloud cover parameters are optimized to address the **rsds** bias. The `tune_box_liq` and `tune_box_liq_asy` parameters are introduced to adjust the relationship between cloud cover (CLC) and relative humidity (RH), and are carefully tuned for operational NWP applications.

The `allow_overcast` factor further refines the dependence of cloud cover on relative humidity. Values less than one increase the average cloud cover. To incorporate seasonal variability, we define a time-dependent monthly variation for `allow_overcast` as follows:

$$\texttt{allow\_overcast}[i] = \textbf{ao} + \textbf{aot4} \cdot aot[i],$$

where **ao** is the mean and $aot[i]$ are the monthly deviations from that mean, $i$ is the index of the month. The deviations are predefined to be positive in summer and negative in winter. This monthly variability is parameterized in the Meta-Model by the mean (**ao**) and the scaling factor ($0.0 \leq$ **aot4** $\leq 1.5$) of the monthly deviations.

https://doi.org/10.5194/egusphere-2025-710
Preprint. Discussion started: 15 April 2025


#### 2.4.4 External data sets

In recent years, new data sets describing the physical properties of soils, surfaces, and the atmosphere have become available. In this study, we investigate the following alternative options:

- `soil_data_base` (**sdb**) describes the physical properties of the soil, provided by FAO (FAO/UNESCO, 1981) [**sdb** $= 0$] and HWSD data (Nachtergaele et al., 2023) [**sdb** $= 1$]. The FAO data set mainly represents sandy soils with a typical spatial resolution of 50 km, while the HWSD data set has a finer resolution of approximately 7 km.

- `type_of_orography` (**oro**) is used to calculate the grid-scale surface elevation and parameters required to parameterize subgrid-scale orographic effects. We use the global NOAA GLOBE data (GLOBE Task Team et al., 1999) [**oro** $= 0$] with a resolution of 30 arcseconds (approximately 1 km), or the Yamazaki-Lab MERIT data (Yamazaki et al., 2017) [**oro** $= 1$] with a finer grid resolution of 3 arcseconds (approximately 100 meters).

- `type_of_aerosols` (**acrf**) parameterizes the feedback of the Cloud Condensation Nuclei Density (CDNC) on cloud formation. For this study, we use Kinne aerosol data (Kinne, 2019) [**acrf** $= 0$], for which CDNC is not available, so we supplement it with MODIS (Schaaf et al., 2021) [**acrf** $= 1$] CDNC data.

### 2.5 Error norm

The standard ICON-CLM model output is generated on an hourly basis (except for **tasmin**, **tasmax** which are daily). To reduce the temporal dimensionality, the daily means for **tas**, **rsds**, **psl**, and **hfls** and the daily sum for **pr_amount** are computed first. To maintain temporal consistency across analyses, an annual cycle of daily values was generated, based on multi-year daily means for each model variable. This approach allows for flexibility in the selection of time spans per variable to accommodate any temporal inconsistencies in observations. For this study, a uniform six-year period from 2003 to 2008 was used across all variables for both model outputs and observations to generate the annual cycle. In addition, to further reduce the dimensionality of the data, monthly mean values of the annual cycle were calculated for each model variable, consolidating the temporal dimension to 12. In principle, there is no need to accumulate the daily values first to generate the monthly averages of the annual cycles, since one can compute the monthly averages first and then compute the multi-year average of the annual cycle. However, this approach generally provides more flexibility, since it allows for more sophisticated distribution-based monthly quantities (e.g., 99$^{\text{th}}$ percentiles of hourly/daily values within climatological month).

To define the error norm we consider horizontal model results $\text{MOD}_{i,j,k,n}$ for variables $v_n$. The indices $i, j$ correspond to horizontal surface spatial dimensions, $k$ is the index of month. The observational data $\text{OBS}_{i,j,k,n}$ were then interpolated to the model grid.

The spatially reduced Root Mean Square Error $\text{RMSE}_{k,n}$ for each variable and time period is defined as

$$\text{RMSE}_{k,n} = \sqrt{\frac{1}{N_x \cdot N_y} \sum_{i,j} \left(\text{MOD}_{i,j,k,n} - \text{OBS}_{i,j,k,n}\right)^2}, \tag{1}$$

https://doi.org/10.5194/egusphere-2025-710
Preprint. Discussion started: 15 April 2025


where $N_x \times N_y$ is the number of horizontal grid points of the simulation domain excluding the lateral boundary relaxation zone. For each variable and month the internal variability (or intrinsic uncertainty) $\sigma_{k,n}$ is defined as the RMSE between the reference and disturbance simulation, where the initial conditions were shifted to 1 month

$$\sigma_{k,n} = \sqrt{\frac{1}{N_x \cdot N_y} \sum_{i,j} \left(\mathrm{MOD}^{\mathrm{ref}}_{i,j,k,n} - \mathrm{MOD}^{\mathrm{dis}}_{i,j,k,n}\right)^2}. \tag{2}$$

In order to obtain a reliable measure of the intrinsic uncertainty of the model, both the reference and disturbance simulations should cover a sufficiently long period, as is the case in the current study with a 6-year period. Otherwise, significant imbalances in the monthly values within the climatological year can occur. The unit less error $\mathrm{ERR}_n$ for each variable is defined as the averaged over time periods RMSE error normalized on internal variability

$$\mathrm{ERR}_n = \frac{1}{N_t} \sum_k \frac{\mathrm{RMSE}_{k,n}}{\sigma_{k,n}}, \tag{3}$$

where $N_t = 12$ is the number of months. The final error norm ERR is defined as the weighted sum of the errors for each variable

$$\mathrm{ERR} = \sum_n c_n \cdot \mathrm{ERR}_n, \ \sum_n c_n = 1. \tag{4}$$

The weights $c_n$ are specified by the user to emphasize the importance of a particular variable and should have the unit sum. The goal of the tuning process is to minimize the error norm (Eq. 4) with respect to the model parameters.

### 2.6 The linear meta-model (LiMMo) approximation

The mean climate can be regarded as a balanced, stable stationary state and thus to be weakly dependent on the model parameters $p_i$. This allows to consider the climate state CLI as a function of a model parameter vector $\boldsymbol{p}$ and to expand $\mathrm{CLI}(\boldsymbol{p})$ in a Taylor series around the reference model solution $\mathrm{CLI}(\boldsymbol{p_0})$. The linear meta model is the first order approximation of the climate state:

$$\mathrm{CLI}(\boldsymbol{p}) \approx \mathrm{CLI}(\boldsymbol{p_0}) + \nabla_{\boldsymbol{p}} \mathrm{CLI}(\boldsymbol{p_0}) \cdot (\boldsymbol{p} - \boldsymbol{p_0}). \tag{5}$$

We rewrite Eq. 5 in the form of a linear regression $\mathrm{REG}_{i,j,k,n}$ for each grid point $(x_i, y_j)$, month $m_k$ and variable $v_n$

$$\mathrm{REG}_{i,j,k,n}(\boldsymbol{p}) = \mathrm{A}_{i,j,k,n} + \sum_{m=1}^{N_c} p_m \cdot \mathrm{K}^m_{i,j,k,n}, \tag{6}$$

where $\mathrm{A}_{i,j,k,n}$ is the shift tensor, $\mathrm{K}^m_{i,j,k,n}$ is the tendency tensor ($m$ is the index of the parameter) and $N_c$ is the number of continuous parameters considered.

To train the linear regression model we present the analytical values of a tendency tensor $\mathrm{K}^m_{i,j,k,n}$ for each $m$, obtained by the method of undefined coefficients by substituting simulations to the general form of linear regression (Eq. 6). After substituting the reference and single parameter disturbance simulation, the value of the tendency tensor is defined as the

https://doi.org/10.5194/egusphere-2025-710
Preprint. Discussion started: 15 April 2025


fraction of the simulation difference to the parameter increment. For example, one can obtain the tensor $\mathrm{K}^{m}_{i,j,k,n}$ corresponding to the parameter $p_m$ as

$$\mathrm{K}^{m}_{i,j,k,n} = \frac{\mathrm{MOD}^{p_m=p_m^{\mathrm{ref}}+\Delta p_m}_{i,j,k,n} - \mathrm{MOD}^{p_m=p_m^{\mathrm{ref}}}_{i,j,k,n}}{\Delta p_m}, \tag{7}$$

since the other parameters except $p_m$ remained unchanged. If more than one linear combination could define the tendency on the parameter, the least-square technique is utilized. After the computation of all tendency tensors, the additional substitution of the reference simulation gives the value of the shift tensor

$$\mathrm{A}_{i,j,k,n} = \mathrm{MOD}^{\mathrm{ref}}_{i,j,k,n} - \sum_{m=1}^{N_c} p_m^{\mathrm{ref}} \cdot \mathrm{K}^{m}_{i,j,k,n}. \tag{8}$$

To account for logical switches, we incorporate constant signals into the Meta-Model (Eq. 6):

$$\mathrm{REG}_{i,j,k,n}(\boldsymbol{p}) = \mathrm{A}_{i,j,k,n} + \sum_{m=1}^{N_c} p_m \cdot \mathrm{K}^{m}_{i,j,k,n} + \sum_{l=1}^{N_b} p_l \cdot \left(\mathrm{MOD}^{p_l=1}_{i,j,k,n} - \mathrm{MOD}^{p_l=0}_{i,j,k,n}\right), \tag{9}$$

where $N_b$ denotes the number of binary (logical) parameters, and each binary parameter $p_l$ can take the values 0 or 1. The reference simulation assumes $p_l = 0$ for all binary parameters. When $p_l = 0$, the logical switch is off, and no additional signal is added, so the Meta-Model would reproduce the state of the reference simulation. The inclusion of binary parameters introduces constant shifts in the result, but does not affect the gradient of the Meta-Model with respect to continuous parameters.

### 2.7 The gradient-based optimization

The core concept behind Meta-Model tuning is to replace the climate model output with a regression approximation in the definition of the error norm (Eq. 4). Due to the simplicity of the Meta-Model, the gradient of the error norm with respect to the model parameters can be computed analytically. The linear regression approximation (Eq. 9) provides the following analytical expression for the gradient with respect to the continuous parameters:

$$\left(\frac{\partial \mathrm{REG}}{\partial \boldsymbol{p}}\right)_m = \mathrm{K}^{m}_{i,j,k,n}. \tag{10}$$

Using the chain rule, the analytical form of the gradient of the error norm (Eq. 4) could be written as

$$\left(\frac{\partial \mathrm{ERR}}{\partial \boldsymbol{p}}\right)_m = \sum_n c_n \frac{1}{N_t \cdot N_x \cdot N_y} \sum_k \frac{1}{\sigma_{k,n} \cdot \mathrm{RMSE}_{k,n}(\boldsymbol{p})} \cdot \sum_{i,j} \left(\mathrm{REG}_{i,j,k,n}(\boldsymbol{p}) - \mathrm{OBS}_{i,j,k,n}\right) \cdot \mathrm{K}^{m}_{i,j,k,n}. \tag{11}$$

The computation of the gradient requires one loop over grid points $(i, j)$, time $(k)$, and model variables $(n)$, making its duration comparable to that of a single norm evaluation $O(N_x \cdot N_y \cdot N_t \cdot N_{\mathrm{vars}})$. The availability of a fast gradient computation procedure allows the use of different optimization methods. This study proposes the implementation of the Limited-memory Broyden-Fletcher-Goldfarb-Shanno with Box constraints (L-BFGS-B) algorithm (Broyden, 1970; Byrd et al., 1995). This method is chosen due to its high convergence speed, being a quasi-Newton method that approximates the Hessian matrix, and its capability to impose constraints on parameter ranges, thereby eliminating nonphysical parameter values during the optimization.

https://doi.org/10.5194/egusphere-2025-710
Preprint. Discussion started: 15 April 2025


In gradient-based optimization, parameter normalization is highly beneficial, as it results in a spherical shape of isolines, improving the convergence rate by avoiding the steep slopes of the objective function

$$p_i^{\text{new}} = \frac{p_i^{\text{old}} - p_i^{\text{min}}}{p_i^{\text{max}} - p_i^{\text{min}}}. \tag{12}$$

The parameter ranges $p_i^{\text{min}}/p_i^{\text{max}}$ are user-defined (Tab. A1 and Tab. A2) and are used for parameter normalization as well as for the box constraints in L-BFGS-B optimization. Applying this linear transformation to the parameters results in the following transformation of the gradient function

$$\left(\frac{\partial}{\partial \boldsymbol{p}} f(p_1^{\text{new}}, ..., p_m^{\text{new}})\right)_i = (p_i^{\text{max}} - p_i^{\text{min}}) \cdot \left(\frac{\partial}{\partial \boldsymbol{p}} f(p_1^{\text{old}}, ..., p_m^{\text{old}})\right)_i.$$

Fig. 3 illustrates the difference in convergence of the proposed method with and without parameter normalization for a specific parameter configuration. The results clearly demonstrate that the normalized approach achieves the same objective function value, but with an order of magnitude fewer iterations (the objective function decrement was set to $10^{-5}$ as the stop criterion in both cases).

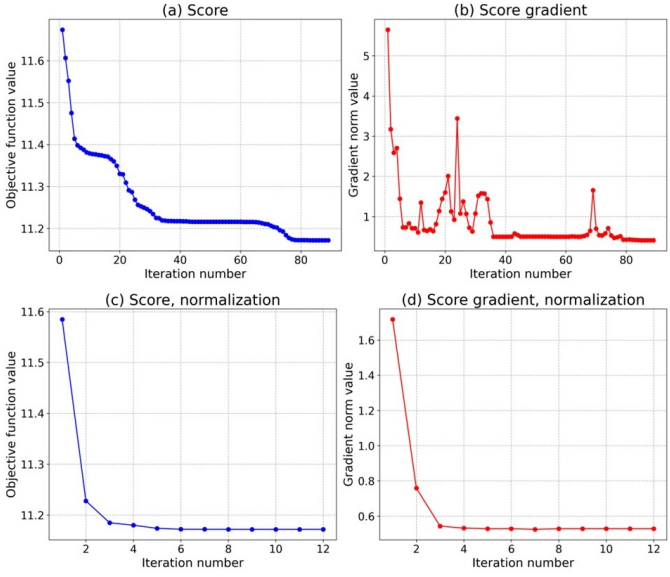


**Figure 3.** Convergence of L-BFGS-B method: score function values without (a) and with (c) parameter normalization, $l2$-norm of score gradient without (b) and with (d) parameter normalization.

The dependence of the solution on the initial conditions can lead to different optimization results. An extremely high optimization speed makes it possible to consider the ensemble of optimization trajectories with the perturbed initial conditions. We propose to select the perturbed initial conditions from the Latin Hypercube vicinity of the reference parameters

$$\left[p_m^{\text{ref}} - \textbf{AMPL} \cdot (p_m^{\text{max}} - p_m^{\text{min}}),\ p_m^{\text{ref}} + \textbf{AMPL} \cdot (p_m^{\text{max}} - p_m^{\text{min}})\right],\ m = \overline{1, N_c}. \tag{13}$$

https://doi.org/10.5194/egusphere-2025-710
Preprint. Discussion started: 15 April 2025


The scaling factor **AMPL** $\in [0, 1]$ defines the amplitude of the perturbation. In the case of the linear regression emulator with a simple RMSE score function, we found no dependence of the result on the initial conditions, as shown in Fig. 4 (we used **AMPL** $= 0.3$ and 15 samples), but this may be different for more advanced statistical emulators or error norm definitions. If a dependence on the initial conditions occurs, one could choose the result with the minimum value of the objective function.

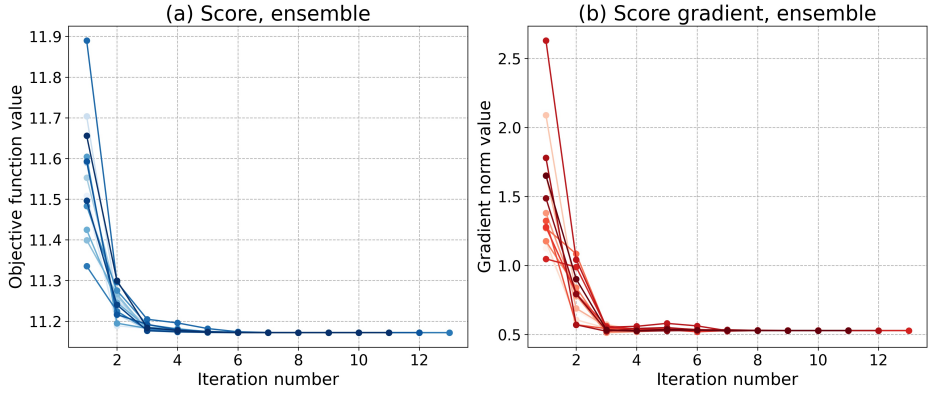


**Figure 4.** Ensemble of 15 optimization trajectories: (a) score function, (b) $l2$-norm of score gradient.

Gradient-based optimization with an analytical representation of the gradient is highly advantageous in terms of performance. The use of linear regression as the statistical emulator results in a linear scaling of the dimensions of the problem (number of variables, parameters, grid points, and time steps), allowing a large number of parameters to be tuned in a reasonable amount of time. The numerical approximation of the gradient is also possible in the case of a more sophisticated statistical emulator or an error norm definition when the analytical expression is not available.

## 3 Results

In this section, we analyze the sensitivity study (section 3.1) and the regression validation (section 3.2) to identify the most influential parameters and to evaluate the performance of the proposed statistical emulator. Subsequently, an example application of LiMMo is presented for a selected parameter set (section 3.3), demonstrating its flexibility in handling varying variable weights. Additionally, the results of an optimization incorporating logical switches (section 3.4) constraints are discussed.

### 3.1 Sensitivity on model parameters

To estimate the sensitivity of the ICON-CLM and consequently of the regression model to the considered parameters, the measure of maximum change is calculated for each prognostic variable. Firstly we compute the maximal function increment $\Delta$REG by separately changing all parameters to their limits

$$\Delta\mathrm{REG}_{i,j,k,n}^{m,\mathrm{min/max}} = \mathrm{REG}_{i,j,k,n}\left(p_1^{\mathrm{ref}},...,p_m^{\mathrm{min/max}},...,p_{N_p}^{\mathrm{ref}}\right) - \mathrm{REG}_{i,j,k,n}\left(p_1^{\mathrm{ref}},...,p_m^{\mathrm{ref}},...,p_{N_p}^{\mathrm{ref}}\right),$$

https://doi.org/10.5194/egusphere-2025-710
Preprint. Discussion started: 15 April 2025


where $N_p$ is the total number of parameters, including continuous and logical ones. The following expression is proposed for the sensitivity benchmark $\mathrm{SENS}_{n,m}$ of the variable $v_n$ to the parameter $p_m$:

$$\mathrm{SENS}_{n,m}^{\min/\max} = \frac{1}{N_T} \cdot \sum_k \frac{1}{\sigma_{k,n}} \cdot \sqrt{\frac{1}{N_x \cdot N_y} \cdot \sum_{i,j} \left(\Delta \mathrm{REG}_{i,j,k,n}^{m,\min/\max}\right)^2} \tag{14}$$

$$\mathrm{SENS}_{n,m} = \max\left(\mathrm{SENS}_{n,m}^{\min},\ \mathrm{SENS}_{n,m}^{\max}\right) \tag{15}$$

The sensitivity measures for all parameters are shown in Fig. 5.

| | tas | rsds | tasmin | tasmax | psl | pr_amount | hfls | Sum |
|---|---|---|---|---|---|---|---|---|
| taw1 | 7.235 | 2.940 | 5.190 | 6.683 | 3.473 | 1.838 | 2.235 | 29.594 |
| taw2 | 0.730 | 0.842 | 0.742 | 0.739 | 0.784 | 0.940 | 0.937 | 5.713 |
| rlh | 2.047 | 1.447 | 2.173 | 2.060 | 2.410 | 1.711 | 5.067 | 16.914 |
| rs | 2.561 | 2.218 | 2.778 | 2.270 | 3.061 | 2.767 | 6.156 | 21.813 |
| rl | 1.761 | 2.577 | 1.837 | 1.809 | 1.749 | 2.132 | 2.145 | 14.010 |
| rsmf | 2.163 | 2.268 | 2.069 | 2.247 | 2.032 | 2.441 | 2.530 | 15.751 |
| crb | 1.668 | 1.328 | 1.576 | 1.682 | 1.269 | 1.445 | 1.698 | 10.667 |
| tbl | 2.694 | 6.281 | 2.733 | 3.019 | 3.143 | 2.595 | 3.018 | 23.482 |
| tbla | 2.329 | 5.797 | 2.100 | 2.811 | 2.835 | 1.733 | 2.318 | 19.924 |
| ao | 3.826 | 7.540 | 2.723 | 4.281 | 3.524 | 2.266 | 3.232 | 27.393 |
| aot4 | 2.179 | 3.241 | 1.761 | 2.274 | 1.590 | 1.590 | 2.016 | 14.652 |
| tkhmin | 2.571 | 1.203 | 3.416 | 1.760 | 1.366 | 1.306 | 1.342 | 12.964 |
| sdb | 2.358 | 0.833 | 4.093 | 1.434 | 0.925 | 0.984 | 1.666 | 12.292 |
| acrf | 0.954 | 1.249 | 0.917 | 0.973 | 0.940 | 0.997 | 0.942 | 6.971 |
| oro | 1.794 | 0.903 | 1.968 | 1.448 | 1.272 | 1.110 | 1.455 | 9.950 |

**Figure 5.** The sensitivity measure of prognostic variables (columns) on model parameters (rows) computed as Eq. 15. The last column gives the sum in the row, which shows the overall sensitivity of the model to the parameter. The numbers are colored in a "blue to red" palette with increasing values.

Overall, the sensitivity results are consistent with theoretical expectations. It is clear that the surface albedo parameterization (**taw1**) is the primary driver of surface air temperature variations (**tas**, **tasmin**, **tasmax**). The heat flux scaling factors (**rlh**, **rs**, **rl**) show sensitivity to both shortwave radiation (**rsds**) and latent heat flux over the sea (**hfls**) with considerable impact on temperature quanities (**tas**, **tasmin** and **tasmax**). The soil resistance parameters (**rsmf** and **crb**) exhibit sensitivity across all model variables. Although optimizing these parameters may not lead to improvements in one variable without affecting others, their inclusion may still be beneficial for optimization.

The cloud cover parameters (**tbl**, **tbla**) and the allow overcast parameterization (**ao**, **aot4**) demonstrate the most pronounced sensitivity to shortwave radiation (**rsds**), as expected. The momentum and vertical diffusion coefficient (**tkhmin**) primarily influence the average (**tas**) and the minimum daily (**tasmin**) temperature with minimal impact on other variables, suggesting opportunities for targeted tuning.

https://doi.org/10.5194/egusphere-2025-710
Preprint. Discussion started: 15 April 2025


The external soil database (**sdb**) primarily affects the mean (**tas**) and the minimum (**tasmin**) temperature. Aerosol type (**acrf**) has a limited effect on shortwave radiation (**rsds**). The orography type (**oro**) has a small effect on all model variables, although it is known to influence wind speed, which is outside the scope of this study.

The proposed sensitivity measure is highly effective for evaluating the impact of parameter changes on model variables and for comparing these impacts quantitatively. This analysis is particularly valuable when considering new parameters, as it helps to assess their influence on model results. Parameters that have a low sensitivity across all model variables (less than 1) could either be removed from the optimization or have the limits of their variation expanded.

### 3.2 Meta-Model validation

To evaluate the accuracy of the linear Meta-Model approximation, several parameter configurations were simulated with ICON-CLM. Some of the most influential parameters identified from the sensitivity analysis (Fig. 5) were selected: **taw1**, **rlh**, **rs**, **rl**, **tbl**, **tbla**, **ao** and **tkhmin**. Test samples were generated by simultaneously varying these parameters within the Latin Hypercube around the minimum and maximum values (see Tab. A1 and Tab. A2). Due to limited computational resources, only the subset of the most sensitive parameters was considered.

A direct comparison between the regression model and the ICON-CLM simulation for different grid points and months is presented in Fig. 6. For the variables **tas**, **tasmin**, **tasmax**, **psl**, and **hfls**, the coefficient of determination ($R^2$) exceeds 0.95 (not shown), indicating a decent approximation by the linear model. The variable **rsds** exhibits some dispersion around the mean but maintains a high determination coefficient. In contrast, precipitation (**pr_amount**) shows the poorest performance, with the Meta-Model occasionally yielding negative precipitation values, which compromises accuracy due to the lack of a constraint enforcing non-negative precipitation amounts.

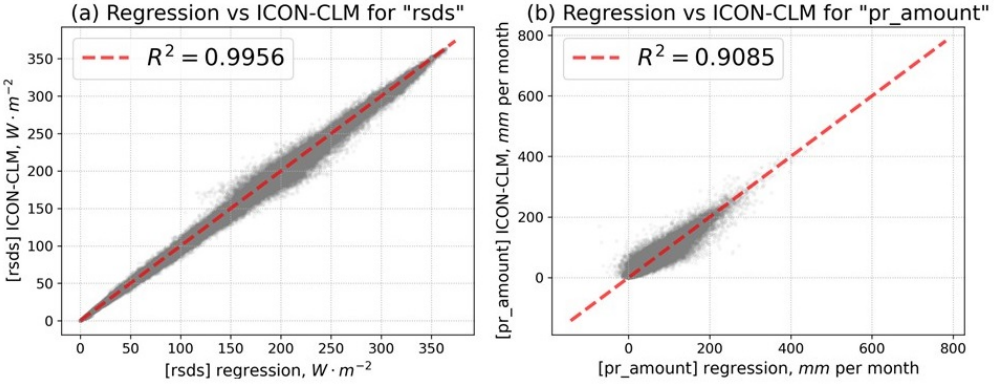


**Figure 6.** The comparison of the regression result (Eq. 6) and the ICON-CLM output for each grid point for training independent setups: (a) monthly mean short wave radiation flux, (b) monthly sum of precipitation. The dashed red line indicates "perfect match", the value of the $R^2$ determination coefficient is given in the label. Every 100th grid point is shown in the plot.

https://doi.org/10.5194/egusphere-2025-710
Preprint. Discussion started: 15 April 2025


The linear approximation error for various variables was assessed by comparing the time-averaged (averaged over all climatological months) RMSEs with the observations (Eq.1), as shown in Fig. 7. The scores of the dynamical simulations and their corresponding Meta-Model approximations are represented by markers of identical shape. Notably, the distance between almost all pairs of markers with the same shape across the axes remains within the range of the intrinsic variability (Eq.2) of the climate model. With a few exceptions, the order of the linear and dynamic errors is largely maintained. This indicates that the optimal linear approximation closely matches the optimal ICON-CLM configuration with a high degree of accuracy, especially when the RMSE is reduced by an amount exceeding the intrinsic variability of the variable under consideration.

This analysis demonstrates the applicability and reliability of the linear approach for representing the dynamical simulations.

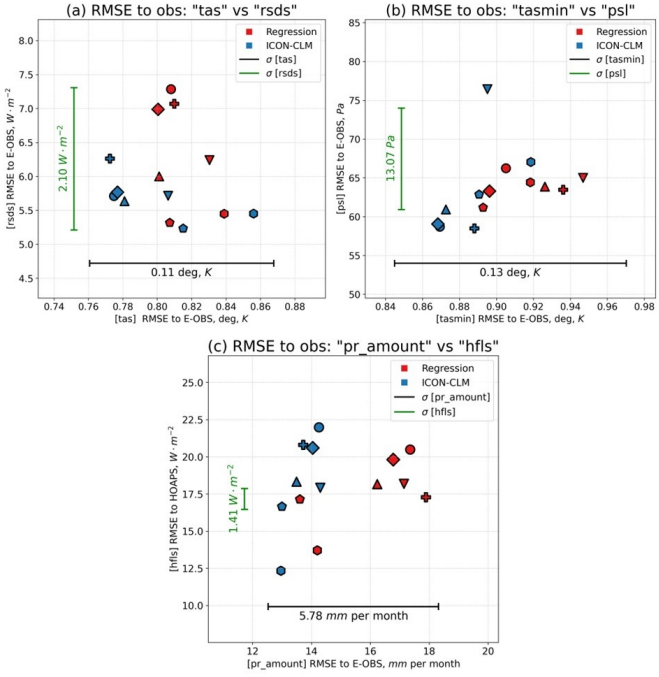


**Figure 7.** The monthly mean RMSEs (Eq. 1) to observations for ICON-CLM simulations (blue markers) and corresponding regression results (red markers). Corresponding dynamical and linear setups are indicated by the same marker shape. The 2003-2008 monthly mean biases are shown for: (a) daily mean 2-meter temperature **tas** versus daily mean short wave flux **rsds**, (b) daily minimum 2-meter temperature **tasmin** versus daily mean sea level pressure **psl**, (c) monthly total precipitation **pr_amount** versus daily mean latent heat flux **hfls**. The 2003-2008 mean internal variabilities of the model (Eq. 2) are shown as horizontal and vertical segments.

### 3.3 Tuning of continuous parameters

LiMMo provides substantial flexibility in the selection of regression parameters for optimization as well as in the weighting of model variables. To systematically evaluate its performance, we fix the set of continuous parameters to the following: **ao**, **aot4**, **taw1**, **taw2**, **rlh**, **rs**, **rl**, **rsmf**, **tbl**, **tbla**, **crb**, and **tkhmin**. Four different weight configurations (Tab.2) for the model variables

https://doi.org/10.5194/egusphere-2025-710
Preprint. Discussion started: 15 April 2025


that define the error norm in Eq.4 are analyzed. As the reference configuration, we used the proposed configuration of ICON for NWP, which defines the shift tensor in Eq. 8. The parameter values of the reference configuration can be found in Tab. 3.

The first configuration, '**equal_weights**', assigns equal weights to all model variables. LiMMo allows to explore the predictive potential of the climate model for specific fields, therefore, two extreme cases are considered: '**tune_prec**' assigns weights exclusively to precipitation, neglecting all other variables, while '**tune_temp**' distributes weights among **tas**, **tasmin**, and **tasmax**. Finally, the '**expert_weights**' configuration reflects weights determined a posteriori by the authors based on an analysis of the optimization results.

| | **tas** | **rsds** | **tasmin** | **tasmax** | **pr_amount** | **psl** | **hfls** |
|---|---|---|---|---|---|---|---|
| **equal_weights** | 1.0 / 7.0 | 1.0 / 7.0 | 1.0 / 7.0 | 1.0 / 7.0 | 1.0 / 7.0 | 1.0 / 7.0 | 1.0 / 7.0 |
| **tune_prec** | 0.0 | 0.0 | 0.0 | 0.0 | 1.0 | 0.0 | 0.0 |
| **tune_temp** | 0.25 | 0.0 | 0.5 | 0.25 | 0.0 | 0.0 | 0.0 |
| **expert_weights** | 0.15 | 0.01 | 0.18 | 0.15 | 0.45 | 0.01 | 0.05 |

**Table 2.** The list of considered weights in the error norn definition (Eq. 4). Each row represents the set of weights of the model quantities (columns).

The performance scores of the model variables (Eq. 3) after optimization are shown in Fig. 8. Note that in the current study we tend to minimize the variable scores (error norms), so the reduced score values demonstrate the better performance. It is evident that the predictability of precipitation is approaching its theoretical limit for the selected set of model parameters, as the optimal score of **pr_amount** in the '**tune_prec**' configuration is only slightly ($\sim 2\%$) lower than that of the reference configuration. It is also worth noting that the initial NWP configuration is already very well tuned for precipitation. Conversely, when optimizing only for temperature variables ('**tune_temp**'), significant error reductions are achievable: a 5% reduction for **tas**, a 12% reduction for **tasmax**, and a 4% reduction for **tasmin**. However, this comes at the cost of a significant imbalance in the surface heat budget, with notable increases in **rsds** (5%) and **hfls** (47%). The quality of **pr_amount** is also badly affected by $15\%$.

The '**equal_weights**' setup demonstrates significant reductions in **rsds** (10%) and **hfls** (25%), but it underperforms the NWP configuration for the key prognostic variables **tas**, **tasmax**, and **pr_amount**. On the other hand, the '**expert_weights**' setup achieves comparable performance to the NWP configuration for most variables, with the exception of **rsds** (1-2% worse) and **tasmax** (2-3% worse). In particular, this setup yields significant improvements in the values of **tasmin** (7%) and **hfls** ($\sim 10\%$). Consequently, the '**expert_weights**' setup can be considered as a viable alternative to the NWP configuration. The optimal values of the considered parameters are listed in the Tab. 3.

### 3.4 Optimization with logical switches

This subsection presents the optimization results obtained using the Meta-Model with incorporated logical switches (Eq. 9). The parameter set is fixed as in the previous subsection, with the '**expert_weights**' weight configuration applied. The study

https://doi.org/10.5194/egusphere-2025-710
Preprint. Discussion started: 15 April 2025


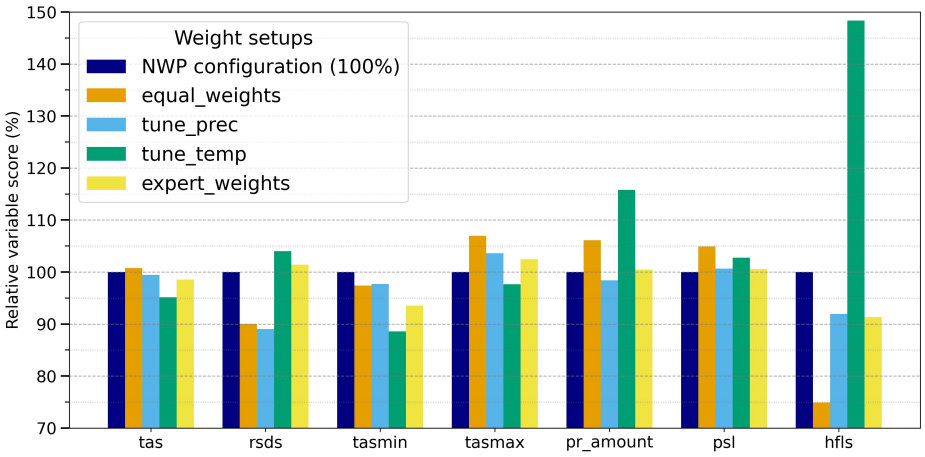


**Figure 8.** Scores of model variables (Eq. 3) normalized by the variable score of NWP configuration (dark blue bars) after optimization with different weights from Tab.2. Note that in the current study we tend to minimize the variable scores (error norms), so the reduced score values demonstrate the better performance.

| | **ao** | **aot4** | **taw1** | **taw2** | **rlh** | **rs** | **rl** | **rsmf** | **tbl** | **tbla** | **crb** | **tkhmin** |
|---|---|---|---|---|---|---|---|---|---|---|---|---|
| **NWP configuration** | 1.000 | 0.000 | 0.000 | 0.000 | 10.000 | 0.800 | 1.000 | 1.000 | 0.050 | 3.250 | 110.000 | 0.600 |
| **equal_weights** | 0.977 | 0.293 | 0.044 | -0.027 | 12.000 | 1.172 | 0.972 | 1.082 | 0.067 | 3.277 | 120.825 | 0.671 |
| **tune_prec** | 0.966 | 0.123 | 0.017 | -0.015 | 11.217 | 0.877 | 0.969 | 1.028 | 0.053 | 3.373 | 111.911 | 0.572 |
| **tune_temp** | 0.980 | 0.819 | 0.114 | -0.103 | 5.000 | 0.605 | 1.089 | 1.070 | 0.040 | 3.147 | 115.625 | 0.566 |
| **expert_weights** | 0.984 | 0.225 | 0.071 | -0.068 | 10.497 | 0.934 | 0.992 | 1.057 | 0.051 | 3.222 | 123.650 | 0.618 |

**Table 3.** The parameter values for the ICON-CLM for the NWP configuration and configurations obtained from LiMMo using different weights from Tab. 2. The rows of the table correspond to the different weights of the variables in the optimization, the columns represent the model parameters.

considers three logical parameters (**sdb**, **acrf** and **oro**), resulting in a total of eight possible configurations. For each configuration, the continuous parameters were optimized. The results are summarized in Fig. 9. The final scores table provides the comprehensive information needed to make an objective decision in selecting the climate model configuration that best meets the user's priorities and interests.

From the Fig.9 one can clearly see the positive effect of more detailed orography on the latent heat flux (**hfls**), as the bias is significantly reduced for all cases when **oro**=1. Overall, updating all external data sets $(\textbf{sdb}, \textbf{acrf}, \textbf{oro}) = (1, 1, 1)$ leads to the most pronounced improvements in precipitation (**pr_amount**) and latent heat flux over sea (**hfls**).

https://doi.org/10.5194/egusphere-2025-710
Preprint. Discussion started: 15 April 2025


| sdb | acrf | oro | tas | rsds | tasmin | tasmax | pr_amount | psl | hfls | Optimal Norm |
|---|---|---|---|---|---|---|---|---|---|---|
| 1 | 1 | 1 | 15.617 | 9.038 | 16.376 | 13.324 | 4.423 | 10.556 | 17.703 | 10.361 |
| 0 | 0 | 0 | 14.666 | 8.825 | 11.855 | 13.813 | 4.440 | 10.145 | 17.485 | 9.468 |
| 0 | 0 | 1 | 14.642 | 9.208 | 12.081 | 13.870 | 4.291 | 10.362 | 16.047 | 9.381 |
| 0 | 1 | 0 | 14.535 | 8.503 | 11.757 | 13.627 | 4.277 | 10.099 | 17.638 | 9.333 |
| 0 | 1 | 1 | 14.507 | 8.874 | 11.986 | 13.679 | 4.112 | 10.296 | 16.169 | 9.236 |
| 1 | 0 | 0 | 14.770 | 8.741 | 12.426 | 13.712 | 4.296 | 9.970 | 18.012 | 9.530 |
| 1 | 0 | 1 | 14.754 | 9.157 | 12.668 | 13.774 | 4.154 | 10.212 | 16.509 | 9.448 |
| 1 | 1 | 0 | 14.657 | 8.419 | 12.339 | 13.540 | 4.122 | 9.925 | 18.159 | 9.397 |
| 1 | 1 | 1 | 14.636 | 8.822 | 12.586 | 13.595 | 3.963 | 10.147 | 16.625 | 9.304 |

**Figure 9.** The variable scores (Eq. 3) for the optimal configurations with different sequences of logical switches. The first row represents the reference NWP configuration. The first three columns describe the sequence of logical switches, while the following columns give the resulting scores for the considered variables. The last column shows the optimal norm (Eq. 4). The values are color-coded with a gradient from red to green, indicating relative deficiency or improvement compared to the corresponding reference values.

## 4 Discussion

The LiMMo optimization strategy demonstrates significant potential for objective calibration. While it quickly and automatically generates optimal parameter values, it requires extensive expert knowledge of the model parameters. The user must define the parameter set, ensure the sensitivity of model outputs to parameter changes, and determine the optimization objective, which is reflected in the assignment of the error norm. The computational efficiency of LiMMo allows for an extensive definition of the error norm. In this study, seven different model quantities are considered, which is a significant increase compared to previous studies. However, for simplicity, we limit the error norm to mean values (root mean square error). From a methodological perspective, it is feasible to include more sophisticated and critical quantities such as extreme precipitation (e.g., the 99$^{th}$ percentile of hourly precipitation over a given period), the diurnal cycle of precipitation, and/or shortwave radiation. Tuning these quantities will be a focus of future research. The current study investigates 10-15 model parameters simultaneously, a scale that was previously unfeasible. However, the linear scalability of the optimization time with respect to the number of parameters allows for a significant expansion of this range, potentially by hundreds of parameters.

Another important aspect, which is beyond the scope of this study, is the monthly weighting of the model variables in the definition of the error norm (Eq. 3, Eq. 4). Given the broad tuning period of six years, the computation of multi-year averages significantly reduces the imbalance of monthly internal variability (Eq. 2), ensuring that the signal-to-noise ratio is approximately equal across months. Therefore, further reduction of temporal dimensionality by considering monthly averages (Eq. 3) is sufficient to treat all months equally. However, for shorter tuning periods, the monthly imbalance in the signal-to-noise ratio may become more pronounced, especially since climate models typically exhibit greater internal variability during the summer months. In such cases, considering monthly averages could lead to an underestimation of the impact of summer

https://doi.org/10.5194/egusphere-2025-710
Preprint. Discussion started: 15 April 2025


months on the model quality score. A more general approach would be to introduce monthly weights for variable errors $f_{k,n}$ (where $k$ is the month index, $n$ is the model variable index), so that the final error norm in the optimization would be

$$\mathrm{ERR} = \sum_n c_n \cdot \sum_k f_{k,n} \cdot \frac{\mathrm{RMSE}_{k,n}}{\sigma_{k,n}}; \sum_k f_{k,n} = 1.$$

This would allow control over the contribution of monthly errors, allowing the weights $f_{k,n}$ to be adjusted to balance their contribution to the overall error norm. For example, one could choose the monthly weights to be inversely proportional to the signal-to-noise ratio for the reference simulation:

$$f_{i,n} \cdot \frac{\mathrm{RMSE}^{\mathrm{ref}}_{i,n}}{\sigma_{i,n}} = f_{j,n} \cdot \frac{\mathrm{RMSE}^{\mathrm{ref}}_{j,n}}{\sigma_{j,n}}, \forall\, i,j; \sum_k f_{k,n} = 1.$$

## 5 Conclusions

The current study introduces a new tool for objective tuning of regional climate models. Building on previous work (Neelin et al., 2010; Bellprat et al., 2015; Avgoustoglou et al., 2022), the LiMMo framework employs a regression-based approximation of climate model outputs. Unlike previous approaches, LiMMo primarily uses a linear regression approximation rather than a quadratic one. This choice is motivated by the cost-effectiveness of building the statistical emulator, as it requires only a linear number of dynamical simulations (at least one for each parameter). Despite its simplicity, the approximation has demonstrated high accuracy when modeling over long periods of time, as evidenced by the 6-year span considered in this study.

A second distinctive feature of LiMMo is the use of a gradient-based method to minimize the error norm relative to observations, in contrast to previously proposed Monte Carlo methods. The combination of a linear Meta-Model with fast gradient-based optimization allows the approach to scale linearly with the number of model quantities and parameters, allowing the simultaneous tuning of dozens of parameters, a task previously infeasible due to time-to-solution constraints.

The LiMMo framework was applied to the state-of-the-art regional climate model ICON-CLM, tuned to the E-OBS and HOAPS observational data sets. A total of 15 model parameters were optimized using 7 model variables that define the distance of the model to the observations. Different optimization objectives were explored by assigning different weights to the model variables in the error norm definition. In addition, optimization was performed for 8 different sequences of 3 logical switches, providing comprehensive insights to objectively select the climate model configuration that best meets the user's priorities.

Please note that the current study is not intended to give any recommendations on the setup of ICON-CLM, but only to demonstrate the capabilities of the proposed LiMMo technique. The final decision of the model configuration should be made after careful and extensive analysis of the model quantities, and LiMMo is only one of the tools that requires expert judgment.

*Code and data availability.* For the experiments, we used the ICON release 2024.07 (https://doi.org/10.35089/WDCC/IconRelease2024.07, ICON partnership (DWD, MPI-M, DKRZ, KIT, C2SM), 2024), which is publicly available under the 3-Clause BSD License; The execution of the job workflow was managed using SPICE - Starter Package for ICON-CLM Experiments, specifically the version 5. 0 released in

https://doi.org/10.5194/egusphere-2025-710
Preprint. Discussion started: 15 April 2025


June 2023 (https://doi.org/10.5281/zenodo.10047021, Rockel and Geyer, 2023), which is publicly available on Zenodo; The ICON-CLM simulations were driven by ERA-5 reanalysis data (https://doi.org/10.24381/cds.143582cf, Hersbach et al., 2020, 2017), with optimization performed using the E-OBS (https://doi.org/10.24381/cds.151d3ec6, Cornes et al., 2018; Copernicus Climate Change Service, Climate Data Store, 2020) and HOAPS (https://doi.org/10.24381/cds.92db7fef, Andersson et al., 2010; Copernicus Climate Change Service, 2022) data sets as reference benchmarks; the Python-based LiMMo software tool (version 1.0) is publicly available on Zenodo (https://doi.org/10.5281/zenodo.14662292, Petrov and Will, 2025). This published software package includes the scripts used to generate the plots in the current manuscript.

*Author contributions.* The concept of employing linear approximation to emulate the climate state was originally proposed by AW. The implementation of gradient-based optimization, its application in Python, and the preparation of the manuscript were carried out by SP. The revision of the paper and the conduction of ICON-CLM simulations was done by BG and AW. All authors have reviewed and approved the final version of the manuscript for publication.

*Competing interests.* The contact author has declared that none of the authors has any competing interests. The funders had no role in the design of the study; in the collection, analysis, or interpretation of the data; in the writing of the manuscript; or in the decision to publish the results.

*Acknowledgements.* The authors would like to thank the members of the CLM community (https://www.clm-community.eu), especially the members of the Evaluation Working Group (WG EVAL), for their valuable discussions, support in running the simulations, and assistance in analyzing the results. We would also like to thank Dr. Stefan Hagemann for reading a draft of the paper and providing valuable comments. We are especially grateful to the German Climate Computing Center (Deutsches Klimarechenzentrum, DKRZ) for providing the computing resources for this study. This work was funded by the project "Updating the data basis for adaptation to climate change in Germany" (BMBF: 01LP2326D).

https://doi.org/10.5194/egusphere-2025-710
Preprint. Discussion started: 15 April 2025


## Appendix A: ICON parameters description

| Section | Parameter | Acronym | Type | Min / Ref / Max value | Description |
|---|---|---|---|---|---|
| 2.4.1 | `tune_albedo_wso(1)` | **taw1** | C | -0.15 / 0.1 / 0.15 | Bare soil albedo correction for soil type 3-6 (sand, sandy-loam, loam, clay-loam) and soil water content `w_so` $< 0.01$. |
| | `tune_albedo_wso(2)` | **taw2** | C | -0.15 / -0.1 / 0.15 | Bare soil albedo correction for soil type 3-6 (sand, sandy-loam, loam, clay-loam) soil water content `w_so` $> 0.02$. |
| | `rlam_heat` | **rlh** | C | 5 / 6.25 / 12 | Scaling factor of the laminar boundary layer for latent and sensible heat flux. Higher values increase the resistance of reduce the sensible heat flux at the surface. |
| | `rat_sea` | **rs** | C | 0.5 / 0.8 / 1.5 | Ratio of laminar scaling factors over sea and land. The larger `rat_sea` the larger the laminar resistance over sea. |
| | `rat_lam` | **rl** | C | 0.7 / 1.0 / 1.3 | Ratio of laminar scaling factors of latent and sensible heat flux over land. The larger `rat_lam` the larger the laminar resistance to latent heat flux over land. |
| | `rsmin_fac` | **rsmf** | C | 0.7 / 1.0 / 1.5 | Scaling factor of class dependent minimum stomata resistance. This preserves the dependency of the resistance on vegetation type. |
| | `cr_bsmin` | **crb** | C | 80 / 110 / 170 | Minimum bare soil evaporation resistance (Schulz and Vogel, 2020) if `itype_evsl=5` (`c_soil` if `itype_evsl=2,3,4`). |
| 2.4.2 | `tkhmin` | **tkhmin** | C | 0.2 / 0.5 / 0.7 | Scaling factor for minimum vertical diffusion coefficient for turbulent heat fluxes at the surface. It is proportional to $R_i^{-2/3}$, with $R_i$ Richardson number. |
| | `tkmmin` | **tkmmin** | C | 0.2 / 0.5 / 1.0 | As `tkhmin` but for momentum. |

**Table A1.** The ICON tuning parameters for **Surface Transfer Scheme** (section 2.4.1) and **Mixing in the Planetary Boundary Layer** (section 2.4.2). The section number with description of parameter is given in the column "Section". The "Parameter" column gives the name of the parameter as used in the ICON model, while the "Acronym" column shows the parameter acronym used in this article. The "Type" column indicates whether the parameter is continuous ("C") or binary ("B"). The "Min/Ref/Max" column represent the minimum, reference, and maximum values for optimization, respectively. The "Description" column provides a brief explanation of each parameter.

https://doi.org/10.5194/egusphere-2025-710
Preprint. Discussion started: 15 April 2025


| Section | Parameter | Acronym | Type | Min / Ref / Max value | Description |
|---|---|---|---|---|---|
| 2.4.3 | `tune_box_liq` | **tbl** | C | 0.04 / 0.05 / 0.1 | Range of relative humidity (RH) for liquid cloud cover (CLC) diagnostics with $1-\textbf{tbla}\cdot\textbf{tbl} \leq \text{RH} \leq 1+\textbf{tbl}$. Higher values increase the cloud cover. |
| | `tune_box_liq_asy` | **tbla** | C | 3.5 / 3.25 / 4.5 | Asymmetry factor for range of RH in liquid cloud cover diagnostics (See `tune_box_liq`). A smaller value is resulting in a smaller range of CLC increase with RH to 1. |
| | `allow_overcast` | **ao** | C | 0.8 / 0.9 / 1.0 | Parameter of the dependency of CLC on RH. A smaller value is resulting in a steeper CLC(RH) increase to 1. |
| | | **aot4** | C | 0 / 1.0 / 1.5 | The amplitude of the annual cycle of monthly deviations of `allow_overcast` from the mean value of **ao**: $\texttt{allow\_overcast}[i] = \textbf{ao} + \textbf{aot4} \cdot aot[i],$ $aot = [-0.02, -0.06, -0.03, 0.02, 0.05, 0.02, 0.02, 0.02, -0.02, -0.04, -0.04, -0.03]$ |
| 2.4.4 | `soil_data_base` | **sdb** | B | 0.0 / 0.0 / 1.0 | Soil type data base. [**sdb** $= 0$]: FAO (FAO/UNESCO, 1981); [**sdb** $= 1$]: HWSD (Nachtergaele et al., 2023). |
| | `type_of_orography` | **oro** | B | 0.0 / 0.0 / 1.0 | Orography data base. [**oro** $= 0$]: NOAA GLOBE 1km resolution (GLOBE Task Team et al., 1999); [**oro** $= 1$]: MERIT 100m resolution (Yamazaki et al., 2017). |
| | `type_of_aerosols` | **acrf** | B | 0.0 / 0.0 / 1.0 | Aerosol climatology data base. [**acrf** $= 0$] Kinne (Kinne, 2019); [**acrf** $= 1$] MODIS (Schaaf et al., 2021). |

**Table A2.** The ICON tuning parameters for **Cloud cover** (section 2.4.3) and **External data sets** (section 2.4.4). The description of the columns is the same as in Tab. A1.

https://doi.org/10.5194/egusphere-2025-710
Preprint. Discussion started: 15 April 2025


## References

Andersson, A., Fennig, K., Klepp, C., Bakan, S., Graßl, H., and Schulz, J.: The Hamburg Ocean Atmosphere Parameters and Fluxes from Satellite Data – HOAPS-3, Earth System Science Data, v.2, 215-234 (2010), 3, https://doi.org/10.5194/essd-2-215-2010, 2010.

Avgoustoglou, E., Carmona, I., Voudouri, A., Levi, Y., Will, A., and Bettems, J.: Calibration of COSMO model in the Central-Eastern Mediterranean area adjusted over the domains of Greece and Israel, Atmospheric Research, 279, 106 362, https://doi.org/10.1016/j.atmosres.2022.106362, 2022.

Bellprat, O., Kotlarski, S., Lüthi, D., Elía, R., Frigon, A., Laprise, R., and Schär, C.: Objective Calibration of Regional Climate Models: Application over Europe and North America, Journal of Climate, 29, 151211135749 001, https://doi.org/10.1175/JCLI-D-15-0302.1, 2015.

Broyden, C. G.: The Convergence of a Class of Double-Rank Minimization Algorithms 2. The New Algorithm, IMA Journal of Applied Mathematics, 6, 222–231, https://doi.org/10.1093/imamat/6.3.222, 1970.

Byrd, R. H., Lu, P., Nocedal, J., and Zhu, C.: A Limited Memory Algorithm for Bound Constrained Optimization, SIAM Journal on Scientific Computing, 16, 1190–1208, https://doi.org/10.1137/0916069, 1995.

Copernicus Climate Change Service: Monthly and 6-hourly total column water vapour over ocean from 1988 to 2020 derived from satellite observations, Copernicus Climate Change Service (C3S) Climate Data Store (CDS), https://doi.org/10.24381/cds.92db7fef, last access: January 2024, 2022.

Copernicus Climate Change Service, Climate Data Store: E-OBS daily gridded meteorological data for Europe from 1950 to present derived from in-situ observations, Copernicus Climate Change Service (C3S) Climate Data Store (CDS), https://doi.org/10.24381/cds.151d3ec6, last access: January 2024, 2020.

Cornes, R., van der Schrier, G., van den Besselaar, E., and Jones, P.: An ensemble version of the E-OBS temperature and precipitation data sets, Journal of Geophysical Research: Atmospheres, 123, 9391–9409, 2018.

FAO/UNESCO: Soil Map of the World, 1:5'000'000, https://www.fao.org/soils-portal/soil-survey/soil-maps-and-databases/faounesco-soil-map-of-the-world/en/, last access: March, 2023, 1981.

GLOBE Task Team, Hastings, D. A., Dunbar, P. K., Elphingstone, G. M., Bootz, M., Murakami, H., Maruyama, H., Masaharu, H., Holland, P., Payne, J., Bryant, N. A., Logan, T. L., Muller, J.-P., Schreier, G., and MacDonald, J. S.: The Global Land One-kilometer Base Elevation (GLOBE) Digital Elevation Model, Version 1.0, https://www.ngdc.noaa.gov/mgg/topo/globe.html, last accessed: March, 2023, 1999.

Gregoire, L., Valdes, P., Payne, A., et al.: Optimal tuning of a GCM using modern and glacial constraints, Climate Dynamics, 37, 705–719, https://doi.org/10.1007/s00382-010-0934-8, 2011.

Hersbach, H., Bell, B., Berrisford, P., Hirahara, S., Horányi, A., Muñoz-Sabater, J., Nicolas, J., Peubey, C., Radu, R., Schepers, D., Simmons, A., Soci, C., Abdalla, S., Abellan, X., Balsamo, G., Bechtold, P., Biavati, G., Bidlot, J., Bonavita, M., De Chiara, G., Dahlgren, P., Dee, D., Diamantakis, M., Dragani, R., Flemming, J., Forbes, R., Fuentes, M., Geer, A., Haimberger, L., Healy, S., Hogan, R., Hólm, E., Janisková, M., Keeley, S., Laloyaux, P., Lopez, P., Lupu, C., Radnoti, G., de Rosnay, P., Rozum, I., Vamborg, F., Villaume, S., and Thépaut, J.-N.: Fifth generation of ECMWF atmospheric reanalyses of the global climate, Copernicus Climate Change Service (C3S) Data Store (CDS), https://doi.org/10.24381/cds.143582cf, last access: June 2024, 2017.

Hersbach, H., Bell, B., Berrisford, P., Hirahara, S., Horányi, A., Muñoz-Sabater, J., Nicolas, J., Peubey, C., Radu, R., Schepers, D., et al.: The ERA5 global reanalysis, Quarterly Journal of the Royal Meteorological Society, 146, 1999–2049, 2020.

ICON partnership (DWD, MPI-M, DKRZ, KIT, C2SM): ICON release 2024.07, World Data Center for Climate (WDCC) at DKRZ, https://doi.org/10.35089/WDCC/IconRelease2024.07, last access: August 2024, 2024.

https://doi.org/10.5194/egusphere-2025-710
Preprint. Discussion started: 15 April 2025


Jacob, D., Petersen, J., Eggert, B., Alias, A., Christensen, O., Bouwer, L., Braun, A., Colette, A., Déqué, M., Georgievski, G., Georgopoulou, E., Gobiet, A., Menut, L., Nikulin, G., Haensler, A., Hempelmann, N., Jones, C., Keuler, K., Kovats, S., and Yiou, P.: EURO-CORDEX: New high-resolution climate change projections for European impact research, Regional Environmental Change, 14, https://doi.org/10.1007/s10113-013-0499-2, 2014.

Kinne, S.: Aerosol radiative effects with MACv2, Atmospheric Chemistry and Physics, 19, 10 919–10 959, https://doi.org/10.5194/acp-19-10919-2019, 2019.

Klocke, D., Brueck, M., Hohenegger, C., and Stevens, B.: Rediscovery of the doldrums in storm-resolving simulations over the tropical Atlantic, Nature Geosci, 10, 891–896, https://doi.org/10.1038/s41561-017-0005-4, 2017.

Mauritsen, T. and Roeckner, E.: Tuning the MPI-ESM1.2 Global Climate Model to Improve the Match With Instrumental Record Warming by Lowering Its Climate Sensitivity, Journal of Advances in Modeling Earth Systems, 12, e2019MS002 037, https://doi.org/10.1029/2019MS002037, 2020.

Morokoff, W. J. and Caflisch, R. E.: Quasi-Monte Carlo Integration, Journal of Computational Physics, 122, 218–230, https://doi.org/10.1006/jcph.1995.1209, 1995.

Nachtergaele, F., Velthuizen, H., Verelst, L., Wiberg, D., Henry, M., Chiozza, F., Yigini, Y., Fischer, G., Tramberend, S., Batjes, N., Montanarella, L., Jones, A., Aksoy, E., Boateng, E., and Shi, X.: Harmonized World Soil Database version 2.0, FAO and IIASA, ISBN 978-92-5-137499-3, https://doi.org/10.4060/cc3823en, 2023.

Neelin, J., Bracco, A., Luo, H., McWilliams, J., and Meyerson, J.: Considerations for parameter optimization and sensitivity in climate models, Proceedings of the National Academy of Sciences of the United States of America, 107, 21 349–54, https://doi.org/10.1073/pnas.1015473107, 2010.

Petrov, S. and Will, A.: LiMMo (Linear Meta-Model optimization for regional climate model), Zenodo, https://doi.org/10.5281/zenodo.14662292, last access: January 2025, 2025.

Pham, T. V., Steger, C., Rockel, B., Keuler, K., Kirchner, I., Mertens, M., Rieger, D., Zängl, G., and Früh, B.: ICON in Climate Limited-area Mode (ICON release version 2.6.1): a new regional climate model, Geoscientific Model Development, 14, 985–1005, https://doi.org/10.5194/gmd-14-985-2021, 2021., 2021.

Rockel, B. and Geyer, B.: SPICE (Starter Package for ICON-CLM Experiments), Zenodo, https://doi.org/10.5281/zenodo.10047021, last access: January 2024, 2023.

Schaaf, C., Wang, Z., and Strahler, A.: MODIS/Terra+Aqua BRDF/Albedo Albedo Daily L3 Global 0.05Deg CMG V061, NASA EOSDIS Land Processes Distributed Active Archive Center, https://doi.org/10.5067/MODIS/MCD43C3.061, last accessed: January, 2024, 2021.

Schulz, J.-P. and Vogel, G.: Improving the Processes in the Land Surface Scheme TERRA: Bare Soil Evaporation and Skin Temperature, Atmosphere, 11, https://doi.org/10.3390/atmos11050513, 2020.

Stevens, B., Fiedler, S., Kinne, S., Peters, K., Rast, S., Müsse, J., Smith, S. J., and Mauritsen, T.: MACv2-SP: a parameterization of anthropogenic aerosol optical properties and an associated Twomey effect for use in CMIP6, Geoscientific Model Development, 10, 433–452, https://doi.org/10.5194/gmd-10-433-2017, 2017.

Yamazaki, D., Ikeshima, D., Tawatari, R., Yamaguchi, T., O'Loughlin, F., Neal, J. C., Sampson, C. C., Kanae, S., and Bates, P. D.: A high-accuracy map of global terrain elevations, Geophysical Research Letters, 44, 5844–5853, https://doi.org/10.1002/2017GL072874, 2017.

Zängl, G.: Adaptive tuning of uncertain parameters in a numerical weather prediction model based upon data assimilation, Quarterly Journal of the Royal Meteorological Society, 149, 2861–2880, https://doi.org/10.1002/qj.4535, 2023.

https://doi.org/10.5194/egusphere-2025-710
Preprint. Discussion started: 15 April 2025


Zängl, G., Reinert, D., Rípodas, P., and Baldauf, M.: The ICON (ICOsahedral Non-hydrostatic) modelling framework of DWD and MPI-M: Description of the non-hydrostatic dynamical core, Quarterly Journal of the Royal Meteorological Society, 141, 563–579, https://doi.org/10.1002/qj.2378, 2015.